processes

MDPI

Article

Estimation and Uncertainty Quantification of Solvent Strength Parameters in Gradient Elution of Chromatography Using Sequential Monte Carlo Method

Ziting Yuan [1], Kensuke Suzuki [1], Yota Yamamoto [1], Tomoyuki Yajima [1] and Yoshiaki Kawajiri [1,2,*]

[1] Department of Material Process Engineering, Nagoya University, Furo-cho 1, Chikusa, Nagoya 464-8603, Aichi, Japan; yuan.ziting.d9@s.mail.nagoya-u.ac.jp (Z.Y.); suzuki.kensuke.k9@s.mail.nagoya-u.ac.jp (K.S.); yajima.tomoyuki@material.nagoya-u.ac.jp (T.Y.)
[2] School of Engineering Science, LUT University, Mukkulankatu 19, 15210 Lahti, Finland
* Correspondence: kawajiri@nagoya-u.jp

Abstract: Gradient elution is a common method for the separation of complex components in chromatography. Strength-dependent models that describe the variation in chromatographic parameters, considering equilibrium and mass transfer under different solution strengths, are essential for the design and optimization of gradient elution. In this study, we proposed several hypothetical models based on experimental data obtained under varying mobile phase ratios in the water–methanol system. The uncertainties in the parameters were quantified using the sequential Monte Carlo (SMC) method with Bayesian inference. Finally, we performed model selection to determine the most appropriate model, utilizing multiple sources of information criteria.

Keywords: chromatography; gradient elution; solvent strength; Bayesian estimation; modeling; uncertainty quantification

check for updates

Academic Editor: Masoud Soroush

Received: 18 December 2024
Revised: 26 December 2024
Accepted: 2 January 2025
Published: 4 January 2025

Citation: Yuan, Z.; Suzuki, K.; Yamamoto, Y.; Yajima, T.; Kawajiri, Y. Estimation and Uncertainty Quantification of Solvent Strength Parameters in Gradient Elution of Chromatography Using Sequential Monte Carlo Method. *Processes* **2025**, *13*, 114. https://doi.org/10.3390/pr13010114

Copyright: © 2025 by the authors. Licensee MDPI, Basel, Switzerland. This article is an open access article distributed under the terms and conditions of the Creative Commons Attribution (CC BY) license (https://creativecommons.org/licenses/by/4.0/).

1. Introduction

High-performance liquid chromatography (HPLC) is a powerful method for separation and purification in various industrial fields, including food, pharmaceuticals, and petrochemicals [1,2]. It is used to separate mixtures dissolved in the mobile phase into their individual components by exploiting the interactions between the components and the solid phase in the column, typically carried out under high pressure [3]. HPLC is widely recognized as a complex process, influenced by numerous factors such as temperature, mobile phase composition, and column length, due to the intricate nature of adsorption equilibria and kinetics. Consequently, careful design and operation are crucial to ensure product safety and improve process economics. Since relying solely on trial-and-error experiments to design the chromatography process is inefficient, modeling serves as a powerful tool to optimize design and operation, significantly reducing material costs and the time required for process development [4].

Gradient elution is a widely used technique as it significantly enhances the separation efficiency of complex mixtures in liquid chromatography. Unlike isocratic elution, which maintains a constant mobile phase composition, gradient elution varies the solvent composition during a batch. This approach enables the effective separation of compounds with diverse polarities and retention characteristics, resulting in improved peak shapes and shorter analysis times. Gradient elution offers the flexibility required to optimize separation conditions, ensuring the best resolution for the components to be separated. By

carefully tailoring the gradient profile, the successful separation of complex samples can be achieved that are difficult to resolve under fixed mobile phase conditions [5,6]. This adaptability makes gradient elution particularly valuable for handling a diverse range of components in a single run, ultimately enhancing the overall efficiency and accuracy of chromatographic separation. This method was widely applied in processes for separating complex components such as proteins [7–15] and DNA [16], Additionally, mathematical models describing these processes were developed [17–20]. The effects of different gradient configurations on separation performance were also investigated [21]. Furthermore, gradient elution is widely utilized in multi-column systems, such as SMB (simulated moving bed) technology [22–24] and multi-column countercurrent solvent gradient purification (MCSGP) [7,25–27], to maximize productivity while minimizing solvent consumption. Gradient elution involves varying the composition of the mobile phase over time to improve the separation of analytes with diverse properties. This approach adds complexity to the separation process, as the interactions between the analytes, the stationary phase, and the mobile phase change dynamically throughout the run. For optimizing the profile of gradient elution, manual optimization or reliance on trial-and-error methods can be highly time-consuming and inefficient [28]. Therefore, efficient optimization techniques for gradient elution are critically needed [29]. However, a method for identifying the most reliable model for chromatographic separation under varying solvent strengths has yet to be established.

The strength of the mobile phase strongly influences the parameters in isotherm and mass transfer models. A stronger solvent has a greater capacity to displace components from the stationary phase, causing them to elute more quickly. This reduces their retention time in the column, resulting in a smaller value for Henry's constant [2]. Conversely, a weaker solvent provides less competition for the stationary phase, allowing for stronger interactions between components and the stationary phase. As a result, components are retained longer, increasing their retention time. Furthermore, solvent strength impacts the equilibrium behavior of components; stronger solvents typically exhibit nearly linear isotherms, whereas weaker solvents can lead to nonlinear behavior [2,30]. However, the behavior of the mass transfer coefficient as a function of solvent strength received comparatively less attention and was only addressed in a limited number of studies [31]. These complex interactions between solvent strength and component behavior must be modeled carefully to ensure accurate predictions and optimal system performance.

Modeling and parameter estimation plays a critical role in the development of chromatographic processes. Building a reliable model depends on accurate parameter estimation methods. A wide range of modeling approaches and analytical solutions were discussed in the literature [30,32–36]. Chromatographic models are typically composed of partial differential equations that describe the key physical and chemical mechanisms in the system. These include the mass transfer of components from the bulk mobile phase to the surface of the solid phase and their diffusion within the porous particles of the stationary phase. Chromatographic models involve several important parameters that are not directly measurable, such as mass transfer coefficients, axial dispersion coefficients, and isotherm parameters. In recent years, many advanced technologies, such as machine learning and artificial intelligence, were applied to the modeling of chromatographic processes; however, there continues to be a lack of methods for parameter estimation with uncertainty quantification [37–39]. The accurate estimation of these parameters is essential and requires both informative experimental data and robust parameter estimation methods. For experimental data, combining pulse injection and breakthrough tests to characterize the adsorption behavior of components at different concentrations provides valuable information for parameter identification [40].

Many approaches were proposed for parameter estimation. Traditional methods include the method of moments [30] and inverse methods that identify the model parameters from the fitting of experimental data [41]. The least-squares method is also commonly used [42], which estimates model parameters for adsorption processes via nonlinear regression [43]. However, these approaches yield only point estimates and do not account for parameter uncertainty, which is crucial for designing robust processes [44]. Traditional methods based on frequentist theory, such as those utilizing the Fisher information matrix, have limitations, particularly for nonlinear models. These methods assume normal distributions and often require extensive datasets, making them less reliable for complex systems [45–47]. In contrast, Bayesian methods can incorporate both experimental data and prior knowledge, making them more effective when data are limited [40]. Bayesian estimation was widely applied in various fields, including biology and chemical processes [48–50], offering a robust framework for parameter estimation under uncertainty.

To efficiently quantify parameter uncertainty, numerical methods such as Markov chain Monte Carlo (MCMC) are commonly used, although they are computationally demanding [51,52]. We recently proposed an alternative approach, a sequential Monte Carlo (SMC) method [53], which offers faster and more flexible computations for parallel implementations. Likelihood tempering, a key feature of the proposed approach, is particularly useful because it gradually modifies the target distribution, allowing the algorithm to explore complex parameter spaces more effectively and avoid getting trapped in local optima. Additionally, SMC has the distinct advantage of being highly amenable to parallelization, enabling significant reductions in computational time compared to MCMC. This parallel capability, combined with the flexibility of automatically updating the tempering factor, enhances the reliability and accuracy of SMC [40,54,55]. These features make SMC a superior option to MCMC for certain complex problems, offering improved computational efficiency and adaptability.

In this study, the SMC method and Bayesian estimation were applied to a chromatographic process considering solvent strength parameters for the first time, enabling the estimation of model parameters while quantifying their uncertainty, which is necessary for designing and optimizing chromatographic processes but inefficient in existing research. Various combinations of adsorption isotherms and solvent strength-dependent models were explored, accounting for the influence of solvent composition not only on adsorption equilibria but also on mass transfer kinetics. Additionally, information criteria were employed to identify the most appropriate models from numerous potential combinations. As an example, phenol in a methanol–water system using an octadecylsilane (ODS) column was studied. To obtain informative data for parameter estimation, experiments were conducted with the component at two different injection volumes and four different ratios of water and methanol. The reliability of the parameter estimation was evaluated based on the posterior probability density distributions of the model parameters. Furthermore, multiple models were compared by information criteria to identify the most appropriate one.

2. Background

2.1. Mathematical Model

A linear driving force model was used in this research [56], which includes the following mass balance equations:

$$\frac{\partial c}{\partial t} + \frac{1-\varepsilon}{\varepsilon}\frac{\partial q}{\partial t} = -v\frac{\partial c}{\partial z} \tag{1}$$

$$\frac{\partial q}{\partial t} = K(q^{eq} - q) \tag{2}$$

where $c[g/L]$ and $q[g/L]$ represent the concentration of the components in liquid and in solid phase, respectively; ε denotes the porosity of the column; $t[s]$ is the time; $z[m]$ denotes axial distance from the column inlet, from 0 to 0.25; $K\left[s^{-1}\right]$ is the overall mass transfer coefficient; $q^{eq}[g/L]$ represents the adsorption equilibrium concentration; and $v[m/s]$ denotes the flow velocity.

2.1.1. Isotherm

Modeling the adsorption isotherm plays an important role in chromatography processes. In this study, two isotherms are investigated, Langmuir and Henry–Langmuir isotherms. The Langmuir type is commonly used as follows:

$$q^{eq} = \frac{Hc}{1+bc} \tag{3}$$

where H [-] represents Henry's constant, and b [L/g] denotes the absorption coefficient.

The Henry–Langmuir type is a hybrid adsorption model that combines the principles of both Henry's law and the Langmuir isotherm. It has both linear and nonlinear terms as shown in the following:

$$q^{eq} = H_1 c + \frac{H_2 c}{1+bc} \tag{4}$$

where H_1[-] and H_2[-] are two kinds of Henry's constants. It may allow for describing adsorption behavior over a wide range of concentrations.

2.1.2. Solvent Strength Parameters

We also model the behavior of the parameter values as they vary with the strength of the solution. Polynomials were first considered as the model because it is a commonly used technique [57], which is favored for its flexibility and computational simplicity. The values of Henry's constant and absorption coefficient are affected by the solvent strength, which are modeled as follows:

$$H_n = \alpha_{0n} + \alpha_{1n} C_{mod} + \alpha_{2n} C_{mod}^2 \tag{5}$$

$$b = \beta_0 + \beta_1 C_{mod} + \beta_2 C_{mod}^2 \tag{6}$$

where the C_{mod} [-] represents the volume fraction of the weaker solvent in the mobile phase, which is water in this study. There, α_{0n}, α_{1n}, α_{2n}, β_0, β_0, and β_0 are solvent strength parameters, and the subscript n = 1,2 is used to distinguish the two Henry constants in the Henry–Langmuir model, Equation (4).

As an alternative approach, we used exponential functions to describe the behavior of Henry's constant and the adsorption coefficient as follows [58]:

$$H_n = \gamma_{1n} C_{mod}^{\gamma_{2n}} \tag{7}$$

$$b = \delta_1 C_{mod}^{\delta_2} \tag{8}$$

where γ_{1n}, γ_{2n}, δ_1, and δ_2 are the solvent strength parameters.

2.1.3. Mass Transfer

In addition to the adsorption equilibrium, the mass transfer rate can be dependent on the solvent strength, which was rarely addressed in past studies. In this study, we considered two different models to describe the relationship between the mass transfer coefficient and the volume fraction of the weaker solvent in the mobile phase C_{mod} [-].

While the influence of modifier concentration could follow a complex functional relationship, introducing too many parameters would complicate their estimation. In one approach, we assumed the mass transfer coefficient to vary linearly with respect to C_{mod} as follows:

$$K = \mu_0 + \mu_1 C_{mod} \tag{9}$$

As an alternative approach, if the influence of the modifier is insignificant, then the mass transfer coefficient can be assumed to be constant as follows:

$$K = \mu_0 \tag{10}$$

where μ_0 and μ_1 are solvent strength parameters.

2.2. Bayesian Inference and SMC Method

Bayesian inference is a statistical technique that utilizes Bayes' theorem to update the probability of an assumption as new evidence or data become available [59]. It provides a framework to incorporate prior knowledge about the parameters to be estimated, along with experimental data, to derive the posterior distributions of these parameters. The theorem is given by the following:

$$P(\theta|y) = \frac{P(y|\theta)P(\theta)}{\int P(y|\theta)P(\theta)d\theta} \tag{11}$$

where θ represents parameter vectors of the models, which require estimation; y is observed data obtained from experiments; $P(\theta)$ is the prior distribution of parameters, which reflects information before experiments; $P(\theta|y)$ is the posterior distribution, which is pursued in this study; and $P(y|\theta)$ is the likelihood function as follows:

$$P(y|\theta) = \prod_{j=1}^{M} \frac{1}{\sqrt{2\pi\sigma^2}} exp\left\{ -\frac{1}{2}\left(\frac{y_j^{model(\theta)} - y_j}{\sigma} \right)^2 \right\} \tag{12}$$

where M represents the dimension of y_j; $y_j^{model(\theta)}$ is the data obtained from the model; and σ is the standard deviation of the observation error. In the denominator of Equation (11), there is an indefinite integral, $\int P(y|\theta)P(\theta)d\theta$, which is not directly computable. Monte Carlo methods are common ways to approximate the posterior distribution.

In this study, a sequential Monte Carlo (SMC) method was implemented. The SMC method approximates the posterior probability density distribution beginning from the prior information via a series of intermediate distributions obtained by likelihood tempering which modifies the numerator of Equation (11) as follows [60]:

$$\pi_i(\theta) = P(y|\theta)^{\gamma_i} P(\theta) \tag{13}$$

where i = 1, 2, 3, . . . N is the stages in the sequence; $\pi_i(\theta)$ is the intermediate distributions in stage i; and γ_i is the tempering parameter which controls the process from prior to posterior distribution. In the above equation, when γ_i = 0, Equation (13) denotes the prior distribution, and when γ_i = 1, it is the posterior distribution. Here, the strategy for updating γ_i is critical; if the increment is too large, particle weights may degenerate; if it is too small, the computation may be unnecessarily slow. In this study, an automatic updating method was employed, which adaptively selects the increment size based on criteria such as the effective sample size (ESS) of the particle weights. This approach ensured a balance between computational efficiency and accuracy [40].

In the SMC method, the intermediate distribution $\pi_i(\theta)$ is approximated by particles with weights. The principle of the SMC is shown in Figure 1. There were four steps in the SMC method utilized in this study. The first step is *initialization*, which starts with particles from the prior distribution with equal weight assigned to all particles; the second step is *mutation*, which mutates all particles to calculate and update the candidates of parameters; the third step is *likelihood calculation*, which calculates the likelihood of each particle; the final step is *resampling*, which redistributes all particles based on the likelihood of them. If the likelihood of a particle is large, the particle is replicated, and if it is small, the particle is eliminated. A detailed description of the method can be found in the previous work of [40].

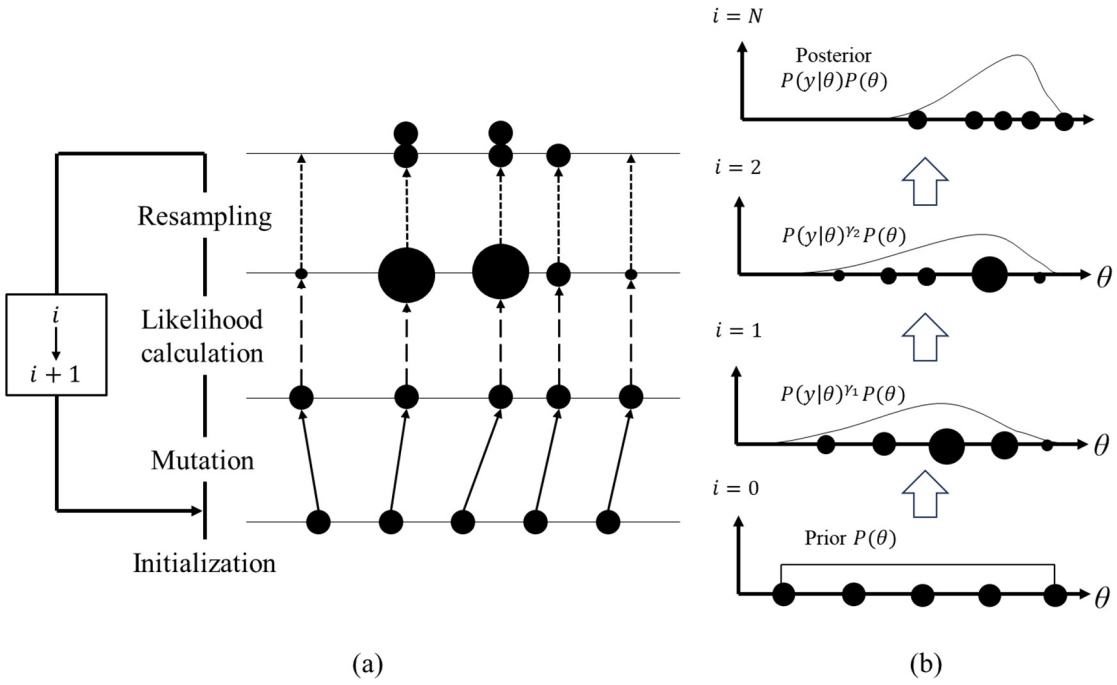


Figure 1. Schematic diagram of SMC. The circles represent particles, and the size of the circles represents the weight of particles. (**a**) Steps in each iteration and (**b**) an overview of iterations.

2.3. Information Criteria for Model Selection

Information criteria are statistical tools used for model selection which allows for the comparison of multiple alternative models. They provide a quantitative framework for evaluating different models and selecting the one that best balances goodness of fit with model complexity. For example, information criteria can distinguish models in situations where adding more parameters improves the model fit to the data but also increases the risk of overfitting. Overfitting is a common problem in modeling, where a model learns the training data too closely, even adapting to noise in the data. As a result, the model performs exceptionally well on the training data but poorly on predictions; in other words, it lacks the ability to generalize new information [61].

Two commonly used information criteria are the Akaike Information Criterion (AIC) [62] and the Bayesian Information Criterion (BIC) [63]. Both criteria balance model fit while penalizing the complexity of the model (i.e., the number of parameters) to prevent overfitting. The smaller the value of an information criterion is, the more appropriate the model is considered to be. The expression of AIC is as follows:

$$AIC = -2\ln(L) + 2K \tag{14}$$

where L is the maximum likelihood of the model, and K is the number of parameters in the model. Similarly, BIC is given as follows:

$$BIC = -2\ln(L) + K\ln(n) \tag{15}$$

where n is the sample size.

3. Methods

3.1. Experiments

All experiments involving phenol were conducted using a high-performance liquid chromatography (HPLC) system. The HPLC system consisted of a degasser (DGU-14A), column oven (CTO-10A), UV-visible spectroscopic detector (SPD-10A), and system controller (SCL-10A), all controlled by the LC Solution software (version 1.21, Shimadzu Corporation, Kyoto, Japan). The column used in this study was prepared by packing a C18 adsorbent (Cosmosil C18-OPN, Nacalai Tesque, Inc., Kyoto, Japan) into a stainless-steel column (Sugiyama Shoji Co., Ltd., Kanagawa, Japan). The column was packed using a slurry method, where the adsorbent particles were dispersed in a mixture of 95% methanol (Fujifilm Wako Pure Chemical Corporation, Osaka, Japan) and 5% pure water. The slurry was loaded into a packer and connected to the column, then pumped into the column at the maximum pump flow rate of 9.99 mL/min to compress the adsorbent particles into a dense and uniform bed. The overall porosity of the column was estimated by injecting uracil as a tracer.

The calibration curve for phenol was obtained by injecting a series of standard solutions at known concentrations (Figure 2). The curve was fitted to the following equation:

$$I_j = Ac_j^2 + Bc_j \tag{16}$$

where I_j is the intensity of phenol measured using a UV detector as a set of discrete-time points at the outlet of the column, and the subscript j is the index for data. In the above equation, A and B are the coefficients of the calibration equation.

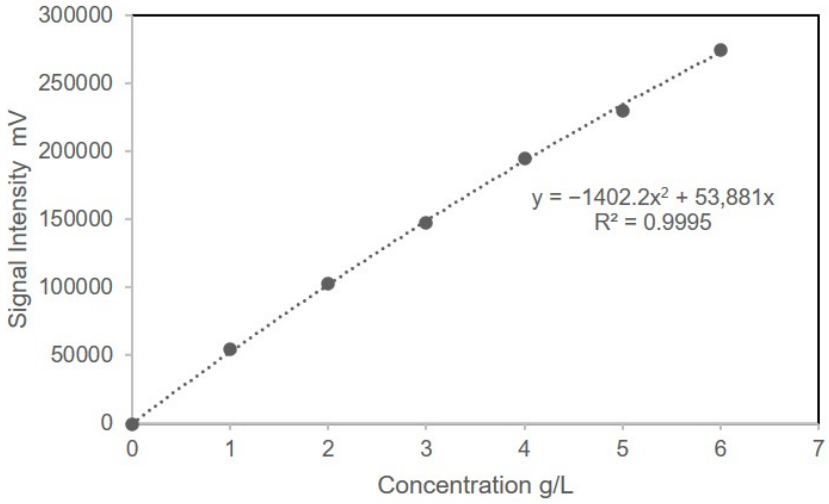


Figure 2. Calibration curve of phenol. The intensity means the magnitude of signal which is proportional to the absorbance of the components.

All experimental conditions and column characteristics are summarized in Table 1(a). The solutions of phenol (Fujifilm Wako Pure Chemical Corporation, Osaka, Japan) in the mobile phase were prepared as the injection samples. Samples were injected using a syringe

and a manual injector equipped with sample loops of two different volumes (Shimadzu Corporation, Kyoto, Japan): 100 µL and 1 mL. Before loading the samples into the sample loop, the loop was flushed with the sample solution at least twice its volume to ensure accuracy.

Table 1. Conditions in obtaining experimental data.

(a) Conditions of Experiments		
Condition	Value	Unit
Length of column	25.0	cm
Diameter of column	1.00	cm
Column porosity	0.705	-
Flow rate	1.50	mL/min
Wavelength of UV detector	256	nm
Temperature	40.0	°C

(b) Labels of Experiments			
	100	1000	µL
Methanol–water = 80:20	A	E	
Methanol–water = 70:30	B	F	
Methanol–water = 60:40	C	G	
Methanol–water = 50:50	D	H	

As shown in Table 1(b), methanol and pure water were mixed in the ratios of 80:20, 70:30, 60:40, and 50:50 by volume to prepare the mobile phases. A series of pulse experiments were conducted using these different mobile phases. The dead volume in the HPLC system was determined to be negligible.

3.2. Solution of the Numerical Model

The partial differential equations (PDEs) (Equations (1)–(4)) described in Section 2.1 were solved by the numerical method of lines [64]. This method discretizes the equations in the spatial domain. In this study, the spatial domain was discretized into 200 finite differences. The package used to solve the set of ordinary differential equations (ODEs) with temporal derivatives numerically was *scipy.integrate.odeint*. To accelerate the expensive computation for the SMC method, a Python Just-In-Time (JIT) compiler Numba was utilized. Furthermore, a library *joblib* in Python was employed for parallel computing to accelerate the computation. The total number of particles was 3000.

The whole computation was performed by a program based on Python 3.6 [65]. The SMC method was implemented on an 11th Gen Intel(R) Core(TM) i9-11900K @ 3.50 GHz with eight cores (16 logical processors), and seven cores were used in this study. The estimation was finished in several hours.

3.3. Combination of Models

In order to find the most accurate model, we combined different isotherms, solvent strength-dependent models, and different mass tran sfer models (I–V), as shown in Table 2.

Table 2. Combination of isotherm and solvent strength-dependent models.

	I	II	III	IV	V
Isotherm	Langmuir Equation (3)	Henry–Langmuir Equation (4)	Langmuir Equation (3)	Henry–Langmuir Equation (4)	Henry–Langmuir Equation (4)
Isotherm parameter dependency on solvent strength	Polynomial Equations (5) and (6)	Polynomial Equations (5) and (6)	Exponential Equations (7) and (8)	Exponential Equations (7) and (8)	Exponential Equations (7) and (8)
Mass transfer coefficient dependency on solvent strength	Linear Equation (9)	Linear Equation (9)	Linear Equation (9)	Linear Equation (9)	Constant Equation (10)

3.4. Estimation Conditions

The prior distributions of all parameters were assumed to be uniform distributions. We obtained initial estimates of solvent strength parameters by the least square method. Based on this estimate, the upper and lower bounds of the uniform distribution were determined. The prior distributions of parameters are shown in Table 3.

Table 3. Prior distributions of all parameters.

Parameters	Prior Distribution
a_{0n}	$U(0,\ 5)$
a_{1n}	$U(0,\ 5)$
a_{2n}	$U(0,\ 5)$
a_{2n}	$U(0,\ 5)$
γ_{1n}	$U(0,\ 5)$
γ_{2n}	$U(0,\ 5)$
μ_0	$U(0,\ 2)$
μ_1	$U(0,\ 2)$
β_0	$U(0,\ 5)$
β_1	$U(0,\ 5)$
β_2	$U(0,\ 5)$
δ_1	$U(0,\ 5)$
δ_2	$U(0,\ 5)$
σ_1	$U(0,\ 50)$
σ_2	$U(0,\ 0.2)$

In addition, we found that the measurement error must be modeled carefully. The measurement error is defined in the following equation:

$$c_{exp,j} = c_j + \varepsilon_j \tag{17}$$

where c_j is the concentration obtained from the model Equations (1)–(4) which is the $y_j^{model(\theta)}$ in Equation (12); $c_{exp,j}$ is the concentration experimentally measured; ε_j is the measurement error; and j is index for time discretization. Here, the measurement error was assumed to follow a normal distribution with variance σ^2:

$$\varepsilon_j \sim N\left(0, \sigma^2\right) \tag{18}$$

In our previous study [40], we found that the assumption of σ^2 being constant led to poor model fit. It was also found that the σ^2 can be a nonlinear function with respect to I_j,

but increasing the parameters to be estimated would make the estimation more difficult. We assumed that the relationship between c_j and σ^2 can be approximated by a linear function as follows:

$$\sigma^2 = \sigma_1^2 + \sigma_2^2 c_j^2 \tag{19}$$

where σ_1 and σ_2 are parameters to be estimated together with other model parameters. In the above equation, σ_1 is the intercept, while σ_2 represents the coefficient for the squared intensity.

4. Results and Discussions

4.1. Fitting of Models and Experiments

The fit between the models and the experimental data was checked. Comparisons of the model I–V with experimental data are shown in Figures 3–7. The fit demonstrates how closely the model aligns with the experimental data, with smaller deviations indicating better model performance. The lines of the models are given by 500 parameter values from the posterior distributions of the parameters randomly, excluding σ_1 and σ_2.

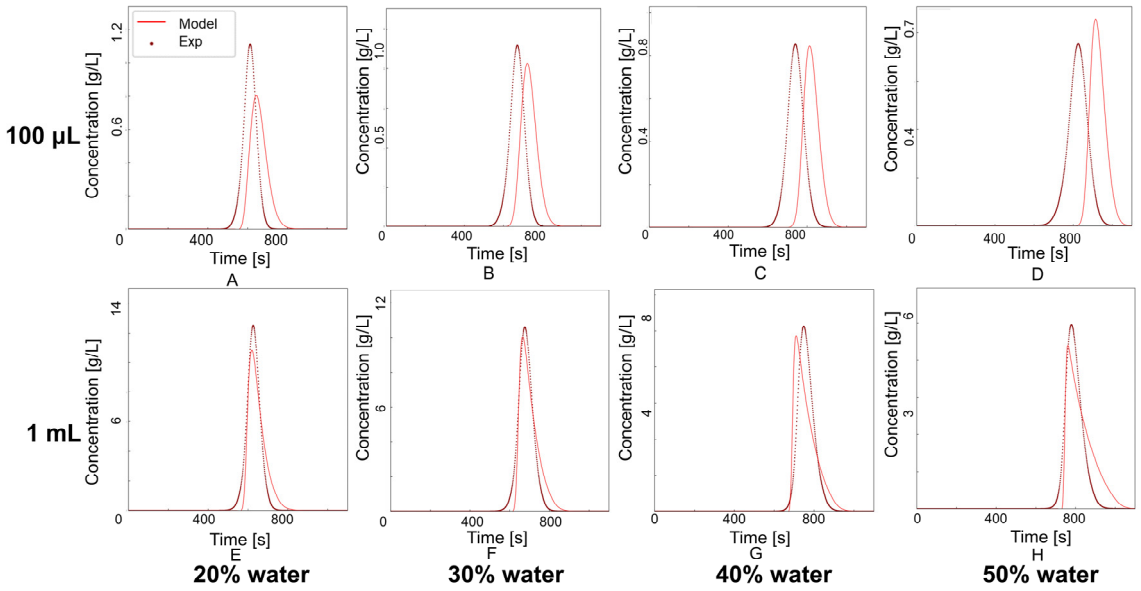


Figure 3. Fitting of the model I (Langmuir with polynomial dependence on solvent strength, and linear dependence of mass transfer coefficient) and experimental data. (**A**) injection volume is 100 µL and mobile phase contains 20% water; (**B**) injection volume is 100 µL and mobile phase contains 30% water; (**C**) injection volume is 100 µL and mobile phase contains 40% water; (**D**) injection volume is 100 µL and mobile phase contains 50% water; (**E**) injection volume is 1 mL and mobile phase contains 20% water; (**F**) injection volume is 1 mL and mobile phase contains 30% water; (**G**) injection volume is 1 mL and mobile phase contains 40% water; and (**H**) injection volume is 1 mL and mobile phase contains 50% water.

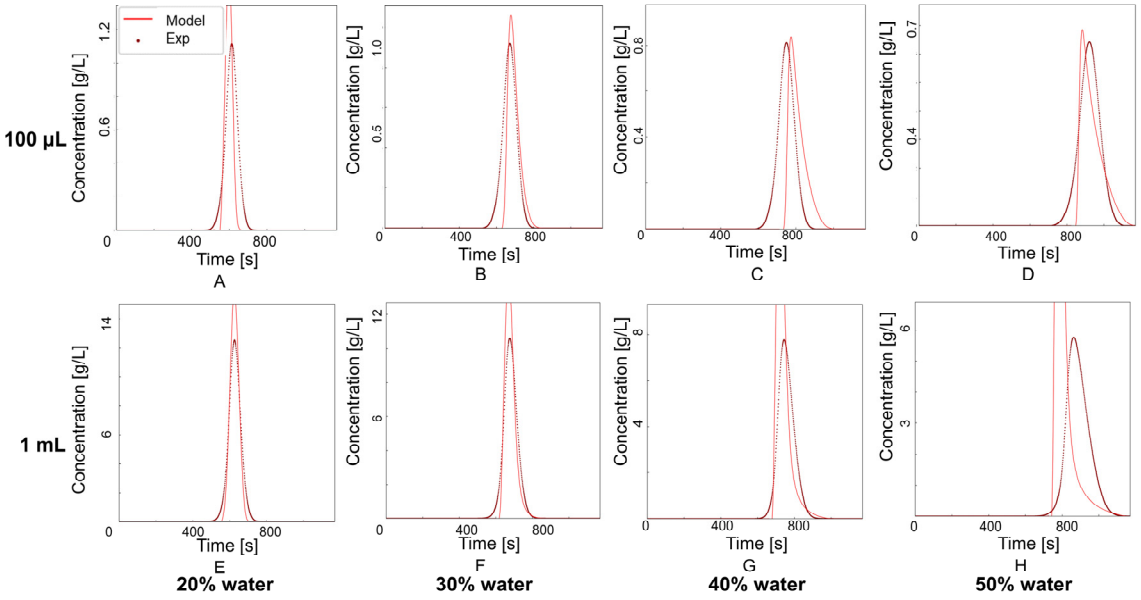


Figure 4. Fitting of the model II (Henry–Langmuir with polynomial dependence on solvent strength, and linear dependence of mass transfer coefficient) and experimental data. (**A**) injection volume is 100 µL and mobile phase contains 20% water; (**B**) injection volume is 100 µL and mobile phase contains 30% water; (**C**) injection volume is 100 µL and mobile phase contains 40% water; (**D**) injection volume is 100 µL and mobile phase contains 50% water; (**E**) injection volume is 1 mL and mobile phase contains 20% water; (**F**) injection volume is 1 mL and mobile phase contains 30% water; (**G**) injection volume is 1 mL and mobile phase contains 40% water; and (**H**) injection volume is 1 mL and mobile phase contains 50% water.

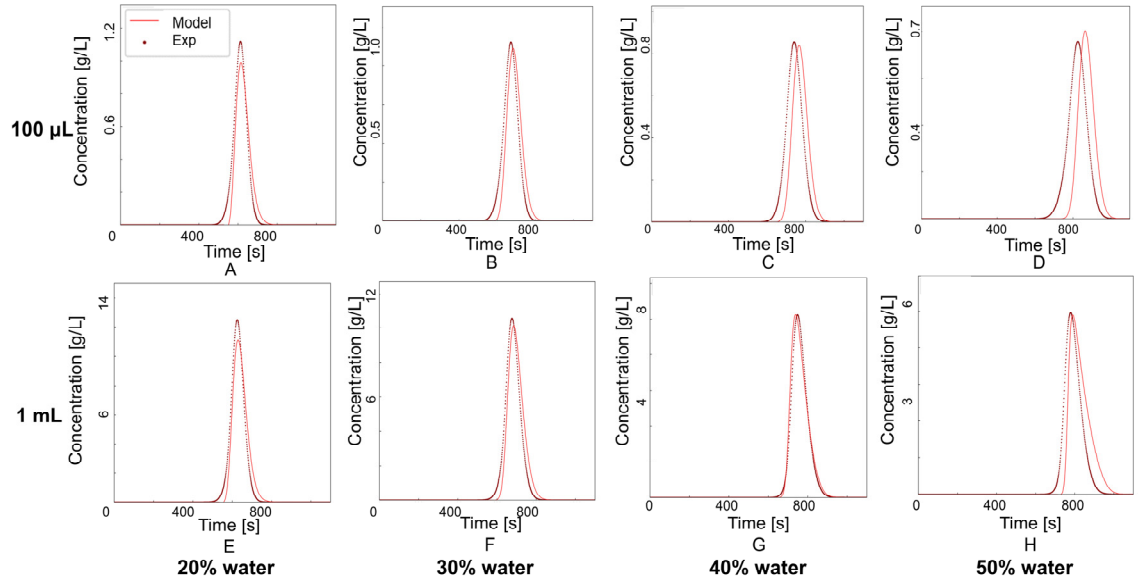


Figure 5. Fitting of the model III (Langmuir with exponential dependence on solvent strength, and linear dependence of mass transfer coefficient) and experimental data. (**A**) injection volume is 100 µL and mobile phase contains 20% water; (**B**) injection volume is 100 µL and mobile phase contains 30% water; (**C**) injection volume is 100 µL and mobile phase contains 40% water; (**D**) injection volume is 100 µL and mobile phase contains 50% water; (**E**) injection volume is 1 mL and mobile phase contains 20% water; (**F**) injection volume is 1 mL and mobile phase contains 30% water; (**G**) injection volume is 1 mL and mobile phase contains 40% water; and (**H**) injection volume is 1 mL and mobile phase contains 50% water.

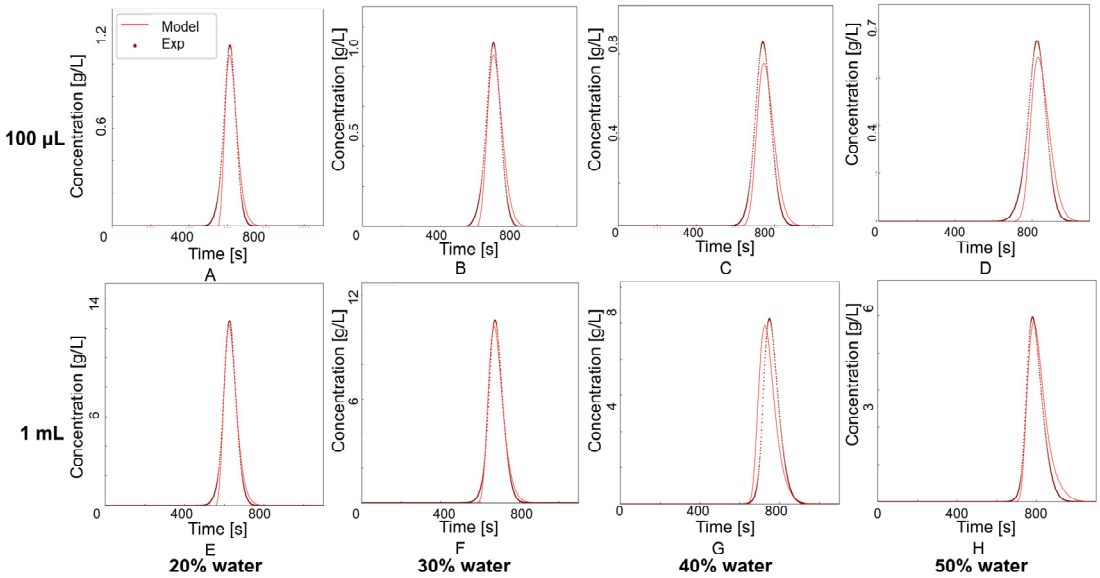


Figure 6. Fitting of the model IV (Henry–Langmuir with exponential dependence on solvent strength, and linear dependence of mass transfer coefficient) and experimental data. (**A**) injection volume is 100 µL and mobile phase contains 20% water; (**B**) injection volume is 100 µL and mobile phase contains 30% water; (**C**) injection volume is 100 µL and mobile phase contains 40% water; (**D**) injection volume is 100 µL and mobile phase contains 50% water; (**E**) injection volume is 1 mL and mobile phase contains 20% water; (**F**) injection volume is 1 mL and mobile phase contains 30% water; (**G**) injection volume is 1 mL and mobile phase contains 40% water; and (**H**) injection volume is 1 mL and mobile phase contains 50% water.

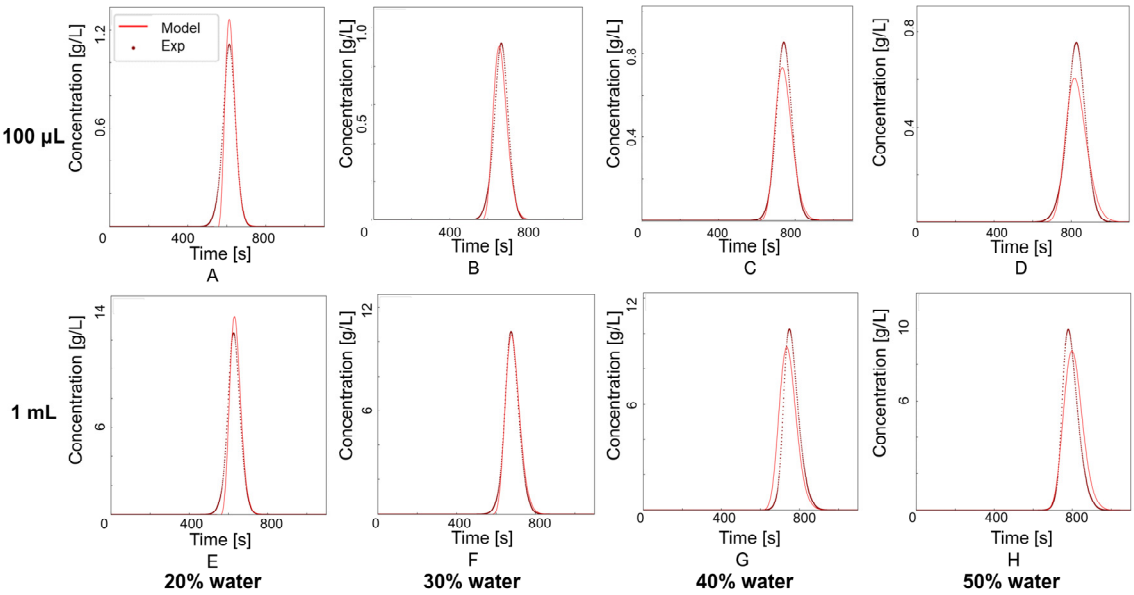


Figure 7. Fitting of the model V (Henry–Langmuir with exponential dependence on solvent strength, and constant mass transfer coefficient) and experimental data. (**A**) injection volume is 100 µL and mobile phase contains 20% water; (**B**) injection volume is 100 µL and mobile phase contains 30% water; (**C**) injection volume is 100 µL and mobile phase contains 40% water; (**D**) injection volume is 100 µL and mobile phase contains 50% water; (**E**) injection volume is 1 mL and mobile phase contains 20% water; (**F**) injection volume is 1 mL and mobile phase contains 30% water; (**G**) injection volume is 1 mL and mobile phase contains 40% water; and (**H**) injection volume is 1 mL and mobile phase contains 50% water.

All models using exponential functions in the isotherm, model III–V (Figures 5–7), performed better than those using polynomial functions, model I and II (Figures 3 and 4). This result suggested that the relationship between solvent strength and isotherm parameters was highly nonlinear. It should be noted that for all exponential models III–V (Figures 5–7), the retention times predicted by the models were very close to the experimental data. This indicated that the Henry constant was relatively straightforward to model. Conversely, for the polynomial models for all polynomial models, model I and II (Figures 3 and 4), the retention times of the models deviated significantly from the experimental data, which shows polynomial models were inappropriate. Additionally, a discrepancy was observed between the model predictions and experimental data in the tail (the latter part of the chromatographic peak) for many models (such as Figure 5H). This suggested that improvements in the modeling of the adsorption coefficient were necessary. In addition, in many models, such as model I and III, the datasets for the injection of 1 mL showed a better fit than that of 100 µL, suggesting that the algorithm may be overly focused on the high-concentration datasets. Applying normalization could potentially improve the overall fit.

Among all models considered in this study, model IV shown in Figure 6 fits the experimental data most accurately, which indicates that the combination of the Henry–Langmuir isotherm adsorption (Equation (4)), linear model for the mass transfer coefficient (Equation (9)) with the exponential model for solvent strength (Equations (7) and (8)), provides the best description of the experimental chromatograms. The Henry–Langmuir model successfully describes chromatograms at both high and low concentrations, likely due to its ability to capture adsorption equilibrium through two independent terms at different levels in the isotherm equation.

Furthermore, the fit of model V shown in Figure 7 is second only to model IV, demonstrating that the assumption of a constant mass transfer coefficient was also reasonable in this study. The results indicated that the mass transfer coefficient was less significantly affected by solvent strength compared to the Henry constant and the adsorption coefficient.

We compared six combination models using the two information criteria, AIC and BIC, as described in Section 2. All models using exponential functions in the isotherm, model III-V (Figures 5–7) had lower values of AIC and BIC than those using polynomial functions, model I and II (Figures 3 and 4). This result may indicate that the relationship between the solvent strength and isotherm parameters are highly nonlinear.

It was found that model IV, the combination of the isotherm exponential model (Equations (7) and (8)), Henry–Langmuir isotherm (Equation (4)) and linear model for the mass transfer coefficient (Equation (9)) had the lowest values of AIC and BIC, as shown in Table 4. It should also be noted that model V, which assumes a constant mass transfer coefficient over the solvent strengths, gave AIC and BIC values that differ by only 1% from those of model IV, which assumes linear dependency of the solvent strength on the mass transfer coefficient. We concluded both models IV and V are both the most appropriate models among the candidates considered in this study (Table 4).

Table 4. AIC and BIC for all models.

Model	AIC	BIC
I	−971.5	−930.9
II	−440.9	−390.4
III	−1600	−1559
IV	−1626	−1576
V	−1613	−1568

4.2. Posterior Distribution of Model Parameters

All parameters of each combination model were estimated as probability density functions. The best-performing models, IV and V, were used as examples for analysis, and the parameter estimation results of other models are shown in Figures S1–S3 of the Supporting Information.

Figure 8 and Table 5 and Figure 9 and Table 6 depict the posterior distributions of all model parameters for models IV and V, respectively. All parameters were estimated as unimodal posterior distributions, and all posterior distributions were significantly sharper than the prior distributions, indicating that the uncertainty of the parameters was effectively reduced. It is worth noting that the distribution of μ_1 includes 0 in Figure 9 for model V (linear dependency of solvent strength on mass transfer coefficient), suggesting that the possibility of the mass transfer coefficient being constant cannot be excluded. This is consistent with the good fit of model V, where the value of μ_1 is fixed to zero. The difficulty in estimating μ_1 highlights a lack of information to uniquely identify this parameter, indicating that modeling the dependency of solvent strength on the mass transfer coefficient remains challenging. Collecting additional data across a broader range of solvent compositions may address this issue. In addition, the parameters for Henry's constant, γ_{11}, γ_{12}, γ_{21}, and γ_{22}, and those for adsorption coefficient, δ_1 and δ_2, obtained by the two models are relatively close, which indicates that the models are reasonable. It was also found that the values of σ_2 for both model IV and V hit the upper bound of the prior distribution, which indicates the upper value needs to be increased. It should be noted that due to the absence of one parameter related to the mass transfer coefficient, model V required slightly less computational time (2 h) compared to model IV (2 h and 45 min). Considering the computational cost and reliability of the models, we believed that both models were acceptable options for describing the system.

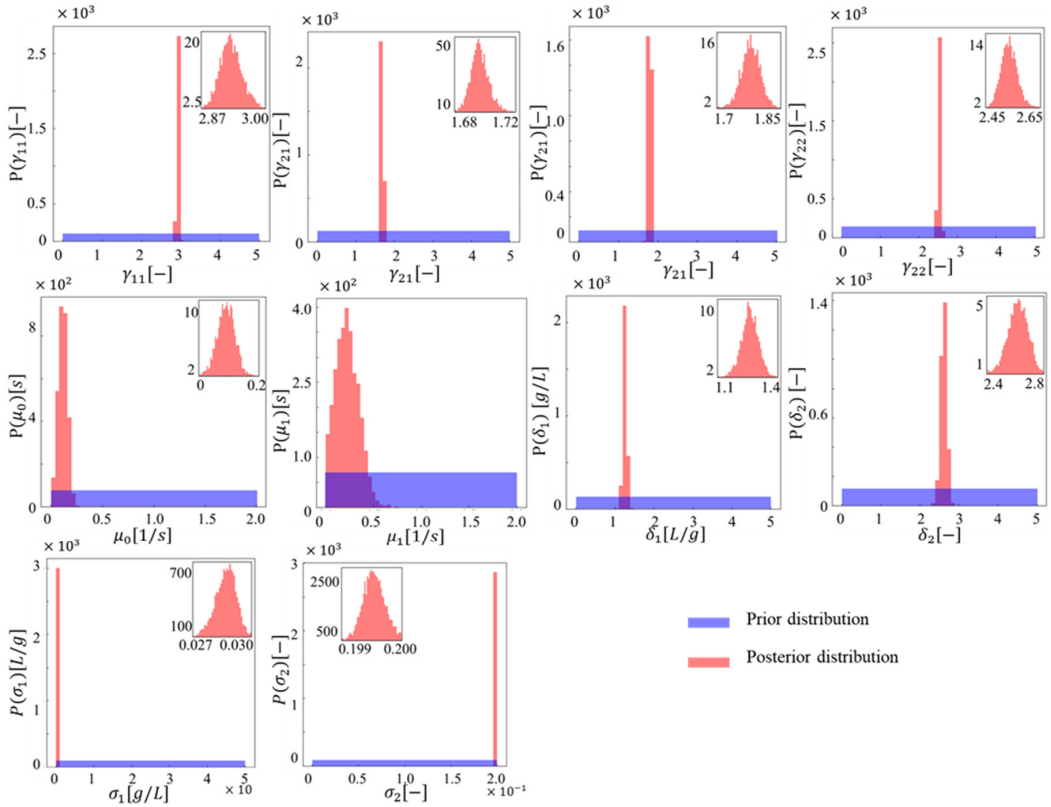


Figure 8. Prior and posterior distributions of all parameters in model IV.

Table 5. Results of estimation of all parameters in model IV.

Parameters	Estimated Value	95% CI	Unit
γ_{11}	2.9307	[2.8892, 2.9801]	-
γ_{12}	1.6935	[1.6779, 1.7138]	-
γ_{21}	1.7988	[1.7387, 1.8534]	-
γ_{22}	2.5404	[2.4801, 2.6015]	-
μ_0	0.1122	[0.0292, 0.1983]	s^{-1}
μ_1	0.2179	[0.0264, 0.4709]	s^{-1}
δ_1	1.2551	[1.1700, 1.3490]	$\frac{g}{L}$
δ_2	2.6277	[2.4600, 2.7557]	-
σ_1	0.0290	[0.0275, 0.0298]	g/L
σ_2	0.1996	[0.1993, 0.1999]	-

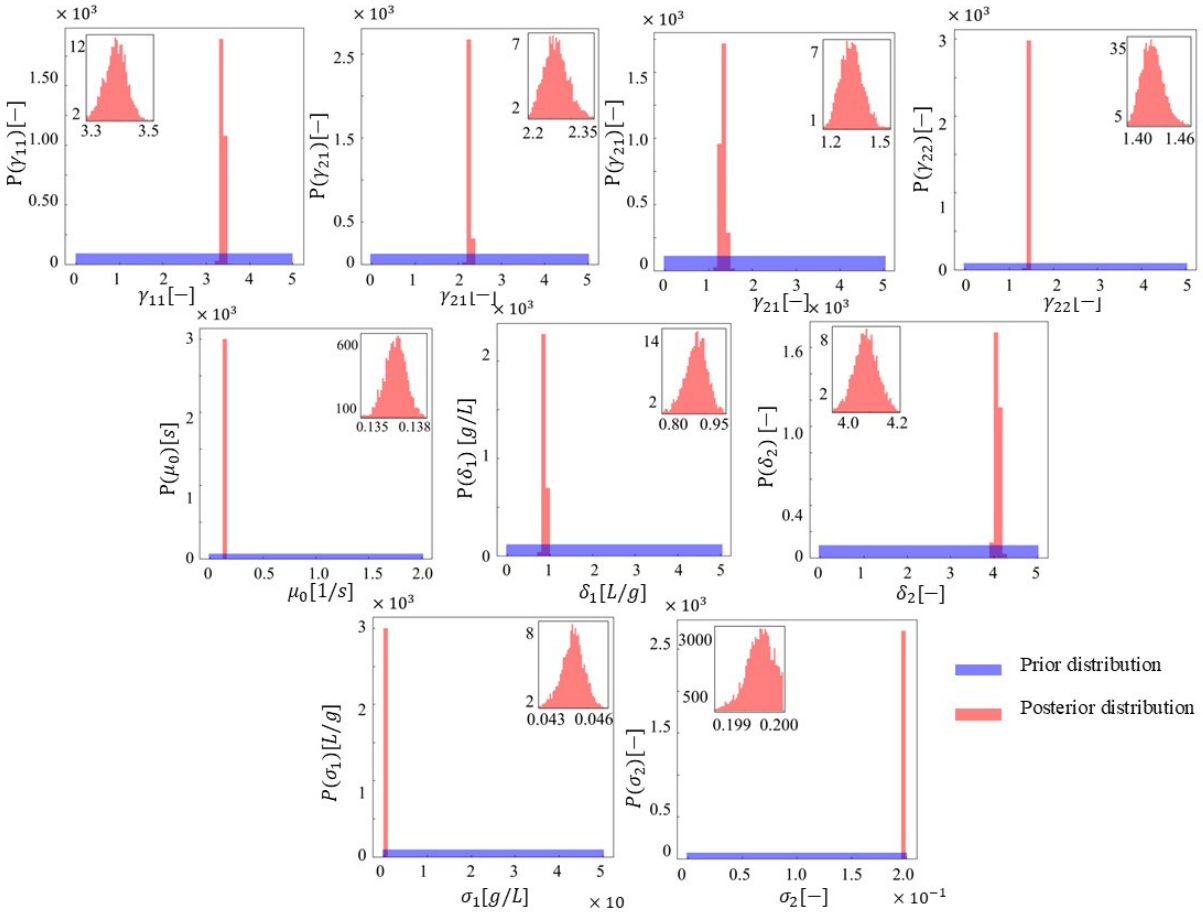


Figure 9. Prior and posterior distributions of all parameters in model V.

Table 6. Results of estimation of all parameters in model V.

Parameters	Estimated Value	95% CI	Unit
γ_{11}	3.3891	[3.3164, 3.4492]	-
γ_{12}	2.2577	[2.2100, 2.3237]	-
γ_{21}	1.3069	[1.2246, 1.4430]	-
γ_{22}	1.4243	[1.4041, 1.4503]	-
μ_0	0.1371	[0.1354, 0.1382]	s^{-1}
δ_1	0.8832	[0.8113, 0.9341]	$\frac{g}{L}$
δ_2	4.0914	[3.9875, 4.1826]	-
σ_1	0.0443	[0.0431, 0.0454]	g/L
σ_2	0.1997	[0.1994, 0.1998]	-

5. Conclusions

In this study, we investigated the modeling of chromatographic parameters varying with solution strength in HPLC gradient elution. Using the adsorption behavior of phenol in methanol–water systems with different ratios as an example, we proposed two hypotheses for the dependence of solvent strength on isotherm parameters. These were combined with commonly used isothermal adsorption models, such as Langmuir and Henry–Langmuir types.

In addition to modeling Henry's constant and adsorption coefficient, we also explored models for the mass transfer coefficient, a topic rarely addressed in previous studies. The best-performing model, identified by minimizing Akaike Information Criterion (AIC) and Bayesian Information Criterion (BIC), was selected based on these two information criteria. Model parameters were successfully estimated using Bayesian inference and the sequential Monte Carlo (SMC) method, and the uncertainty of the parameters was effectively quantified.

Despite these advancements, several issues remain for future research. One key challenge is understanding the behavior of the axial diffusion coefficient under varying solvent strengths. The strong correlation between the axial diffusion coefficient and the mass transfer coefficient slows the convergence of the proposed algorithm. Additionally, employing a wider range of mobile phase strengths could further improve parameter estimation.

Future studies should also investigate more complex molecules, such as proteins, and alternative gradient elution methods, such as linear gradient elution. However, addressing these challenges will likely require larger experimental datasets and may increase computational costs. In addition, we used only a methanol–water system as a case study to explore the dependence of model parameters on solution strength, which should be tested in other systems.

Supplementary Materials: The following supporting information can be downloaded at: https://www.mdpi.com/article/10.3390/pr13010114/s1.

Author Contributions: Z.Y.: Investigation, Methodology, Software, Data curation, Visualization, Formal analysis, Writing—original draft. K.S.: Investigation, Methodology, Software. Y.Y.: Methodology, Software. T.Y.: Investigation, Software, Supervision. Y.K.: Conceptualization, Funding acquisition, Project administration, Supervision, Writing—review and editing. All authors have read and agreed to the published version of the manuscript.

Funding: This study was supported by the Japan Society for the Promotion of Science (JSPS) Grants-in-Aid for Scientific Research, Grant Number JP21H01703.

Data Availability Statement: The data supporting the conclusions of this study can be obtained from the corresponding author.

Conflicts of Interest: The authors declare that they have no known competing financial interests or personal relationships that could have appeared to influence the work reported in this paper.

References

1. Nollet, L.M.L.; Toldrá, F. *Food Analysis by HPLC*; CRC Press: Boca Raton, FL, USA, 2012; Volume 100, ISBN 1439830843.
2. Snyder, L.R.; Kirkland, J.J.; Dolan, J.W. *Introduction to Modern Liquid Chromatography*; John Wiley & Sons: Hoboken, NJ, USA, 2011; ISBN 1118210395.
3. Schmidt-Traub, H.; Schulte, M.; Seidel-Morgenstern, A. *Preparative Chromatography*; John Wiley & Sons: Hoboken, NJ, USA, 2020; ISBN 3527344861.
4. Hahn, T.; Sommer, A.; Osberghaus, A.; Heuveline, V.; Hubbuch, J. Adjoint-Based Estimation and Optimization for Column Liquid Chromatography Models. *Comput. Chem. Eng.* **2014**, *64*, 41–54. [CrossRef]

5. Blumberg, L.M. Theory of Gradient Elution Liquid Chromatography with Linear Solvent Strength: Part 1. Migration and Elution Parameters of a Solute Band. *Chromatographia* **2014**, *77*, 179–188. [CrossRef]
6. Nakamura, H.; Konishi, T.; Kamada, M. Evaluation of Gradient Elution System for High Performance Liquid Chromatography Based on Separation Behavior of Proteins. *Anal. Sci.* **1989**, *5*, 521–524. [CrossRef]
7. Aumann, L.; Morbidelli, M. A Continuous Multicolumn Countercurrent Solvent Gradient Purification (MCSGP) Process. *Biotechnol. Bioeng.* **2007**, *98*, 1043–1055. [CrossRef] [PubMed]
8. Chen, C.; Ando, K.; Yoshimoto, N.; Yamamoto, S. Linear Flow-velocity Gradient Chromatography—An Efficient Method for Increasing the Process Efficiency of Batch and Continuous Capture Chromatography of Proteins. *Biotechnol. Bioeng.* **2021**, *118*, 1262–1272. [CrossRef]
9. De Luca, C.; Felletti, S.; Macis, M.; Cabri, W.; Lievore, G.; Chenet, T.; Pasti, L.; Morbidelli, M.; Cavazzini, A.; Catani, M. Modeling the Nonlinear Behavior of a Bioactive Peptide in Reversed-Phase Gradient Elution Chromatography. *J. Chromatogr. A* **2020**, *1616*, 460789. [CrossRef] [PubMed]
10. De Luca, C.; Felletti, S.; Lievore, G.; Chenet, T.; Morbidelli, M.; Sponchioni, M.; Cavazzini, A.; Catani, M. Modern Trends in Downstream Processing of Biotherapeutics through Continuous Chromatography: The Potential of Multicolumn Countercurrent Solvent Gradient Purification. *TrAC Trends Anal. Chem.* **2020**, *132*, 116051. [CrossRef]
11. Ishihara, T.; Yamamoto, S. Optimization of Monoclonal Antibody Purification by Ion-Exchange Chromatography: Application of Simple Methods with Linear Gradient Elution Experimental Data. *J. Chromatogr. A* **2005**, *1069*, 99–106. [CrossRef]
12. Müller-Späth, T.; Aumann, L.; Melter, L.; Ströhlein, G.; Morbidelli, M. Chromatographic Separation of Three Monoclonal Antibody Variants Using Multicolumn Countercurrent Solvent Gradient Purification (MCSGP). *Biotechnol. Bioeng.* **2008**, *100*, 1166–1177. [CrossRef] [PubMed]
13. Yamamoto, S.; Okada, T.; Abe, M.; Yoshimoto, N. Peak Spreading in Linear Gradient Elution Chromatography with a Thin Monolithic Disk. *J. Chromatogr. A* **2011**, *1218*, 2460–2466. [CrossRef] [PubMed]
14. Yamamoto, S.; Nomura, M.; Sano, Y. Resolution of Proteins in Linear Gradient Elution Ion-Exchange and Hydrophobic Interaction Chromatography. *J. Chromatogr. A* **1987**, *409*, 101–110. [CrossRef] [PubMed]
15. Yamamoto, S.; Nomura, M.; Sano, Y. Adsorption Chromatography of Proteins: Determination of Optimum Conditions. *AIChE J.* **1987**, *33*, 1426–1434. [CrossRef]
16. Yamamoto, S. Plate Height Determination for Gradient Elution Chromatography of Proteins. *Biotechnol. Bioeng.* **1995**, *48*, 444–451. [CrossRef] [PubMed]
17. Yamamoto, S.; Nakanishi, K.; Matsuno, R.; Kamikubo, T. Ion Exchange Chromatography of Proteins—Prediction of Elution Curves and Operating Conditions. I. Theoretical Considerations. *Biotechnol. Bioeng.* **1983**, *25*, 1465–1483. [CrossRef]
18. Yamamoto, S.; Nomura, M.; Sano, Y. Preparative Chromatography of Proteins: Design Calculation Procedure for Gradient and Stepwise Elution. *J. Chromatogr. A* **1990**, *512*, 89–100. [CrossRef]
19. Yamamoto, S.; Kita, A. Theoretical Background of Short Chromatographic Layers: Optimization of Gradient Elution in Short Columns. *J. Chromatogr. A* **2005**, *1065*, 45–50. [CrossRef]
20. Staby, A.; Rathore, A.S.; Ahuja, S. *Preparative Chromatography for Separation of Proteins*; John Wiley & Sons: Hoboken, NJ, USA, 2017; ISBN 9781119031109.
21. Kim, T.K.; Bham, A.A.; Fioretti, I.; Angelo, J.; Xu, X.; Ghose, S.; Morbidelli, M.; Sponchioni, M. Role of the Gradient Slope during the Product Internal Recycling for the Multicolumn Countercurrent Solvent Gradient Purification of PEGylated Proteins. *J. Chromatogr. A* **2023**, *1692*, 463868. [CrossRef] [PubMed]
22. Abel, S.; Mazzotti, M.; Morbidelli, M. Solvent Gradient Operation of Simulated Moving Beds: 2. Langmuir Isotherms. *J. Chromatogr. A* **2004**, *1026*, 47–55. [CrossRef] [PubMed]
23. Antos, D.; Seidel-Morgenstern, A. Two-Step Solvent Gradients in Simulated Moving Bed Chromatography: Numerical Study for Linear Equilibria. *J. Chromatogr. A* **2002**, *944*, 77–91. [CrossRef] [PubMed]
24. Aumann, L.; Morbidelli, M. A Semicontinuous 3-column Countercurrent Solvent Gradient Purification (MCSGP) Process. *Biotechnol. Bioeng.* **2008**, *99*, 728–733. [CrossRef] [PubMed]
25. De Luca, C.; Lievore, G.; Bozza, D.; Buratti, A.; Cavazzini, A.; Ricci, A.; Macis, M.; Cabri, W.; Felletti, S.; Catani, M. Downstream Processing of Therapeutic Peptides by Means of Preparative Liquid Chromatography. *Molecules* **2021**, *26*, 4688. [CrossRef] [PubMed]
26. De Luca, C.; Felletti, S.; Lievore, G.; Buratti, A.; Vogg, S.; Morbidelli, M.; Cavazzini, A.; Catani, M.; Macis, M.; Ricci, A. From Batch to Continuous Chromatographic Purification of a Therapeutic Peptide through Multicolumn Countercurrent Solvent Gradient Purification. *J. Chromatogr. A* **2020**, *1625*, 461304. [CrossRef] [PubMed]
27. Schenkel, B.; Aumann, L.; Stroehlein, G.; Morbidelli, M. Protein Peptide Purification Using the Multicolumn Countercurrent Solvent Gradient Purification (MCSGP) Process. *BioPharm Int.* **2009**, *22*, 46–53.
28. Jandera, P.; Churacek, J. *Gradient Elution in Column Liquid Chromatography: Theory and Practice*; Elsevier: Amsterdam, The Netherlands, 1985; ISBN 0080858341.

29. Snyder, L.R.; Dolan, J.W. *High-Performance Gradient Elution: The Practical Application of the Linear-Solvent-Strength Model*; John Wiley & Sons: Hoboken, NJ, USA, 2006; ISBN 0470055510.
30. Guiochon, G.; Felinger, A.; Shirazi, D.G. *Fundamentals of Preparative and Nonlinear Chromatography*; Elsevier: Amsterdam, The Netherlands, 2006; ISBN 0080457223.
31. Pfister, D.; Morbidelli, M. Mass Transfer Coefficients Determination from Linear Gradient Elution Experiments. *J. Chromatogr. A* **2015**, *1375*, 42–48. [CrossRef]
32. Bellot, J.C.; Condoret, J.S. Liquid Chromatography Modelling: A Review. *Process Biochem.* **1991**, *26*, 363–376. [CrossRef]
33. Guiochon, G. Preparative Liquid Chromatography. *J. Chromatogr. A* **2002**, *965*, 129–161. [CrossRef] [PubMed]
34. Klatt, K. Modellierung Und Effektive Numerische Simulation von Chromatographischen Trennprozessen Im SMB-Betrieb. *Chemie Ing. Tech.* **1999**, *71*, 555–566. [CrossRef]
35. Ruthven, D.M. *Principles of Adsorption and Adsorption Processes*; John Wiley & Sons: Hoboken, NJ, USA, 1984; ISBN 0471866067.
36. Tallvod, S.; Andersson, N.; Nilsson, B. Automation of Modeling and Calibration of Integrated Preparative Protein Chromatography Systems. *Processes* **2022**, *10*, 945. [CrossRef]
37. Zang, W.; Sharma, R.; Li, M.W.-H.; Fan, X. Retention Time Trajectory Matching for Peak Identification in Chromatographic Analysis. *Sensors* **2023**, *23*, 6029. [CrossRef]
38. Zou, T.; Yajima, T.; Kawajiri, Y. A parameter estimation method for chromatographic separation process based on physics-informed neural network. *J. Chromatogr. A* **2024**, *1730*, 465077. [CrossRef]
39. Singh, Y.R.; Shah, D.B.; Kulkarni, M.; Patel, S.R.; Maheshwari, D.G.; Shah, J.S.; Shah, S. Current Trends in Chromatographic Prediction Using Artificial Intelligence and Machine Learning. *Anal. Methods* **2023**, *15*, 2785–2797. [CrossRef] [PubMed]
40. Yuan, Z.; Yamamoto, Y.; Yajima, T.; Kawajiri, Y. Estimation and Statistical Analysis of Model Parameters Using Sequential Monte Carlo for Phenol and P-Cresol Separation. *J. Chromatogr. A* **2023**, *1688*, 463703. [CrossRef]
41. Lietta, E.; Pieri, A.; Cardillo, A.G.; Vanni, M.; Pisano, R.; Barresi, A.A. An Experimental and Modeling Combined Approach in Preparative Hydrophobic Interaction Chromatography. *Processes* **2022**, *10*, 1027. [CrossRef]
42. Maeder, M.; Zuberbühler, A.D. Nonlinear Least-Squares Fitting of Multivariate Absorption Data. *Anal. Chem.* **1990**, *62*, 2220–2224. [CrossRef]
43. Osmari, T.A.; Gallon, R.; Schwaab, M.; Barbosa-Coutinho, E.; Severo, J.B.; Pinto, J.C. Statistical Analysis of Linear and Non-Linear Regression for the Estimation of Adsorption Isotherm Parameters. *Adsorpt. Sci. Technol.* **2013**, *31*, 433–458. [CrossRef]
44. Miller, D.C.; Syamlal, M.; Mebane, D.S.; Storlie, C.; Bhattacharyya, D.; Sahinidis, N.V.; Agarwal, D.; Tong, C.; Zitney, S.E.; Sarkar, A.; et al. Carbon Capture Simulation Initiative: A Case Study in Multiscale Modeling and New Challenges. *Annu. Rev. Chem. Biomol. Eng.* **2014**, *5*, 301–332. [CrossRef]
45. Brestrich, N.; Hahn, T.; Hubbuch, J. Application of Spectral Deconvolution and Inverse Mechanistic Modelling as a Tool for Root Cause Investigation in Protein Chromatography. *J. Chromatogr. A* **2016**, *1437*, 158–167. [CrossRef]
46. Huuk, T.C.; Hahn, T.; Doninger, K.; Griesbach, J.; Hepbildikler, S.; Hubbuch, J. Modeling of Complex Antibody Elution Behavior under High Protein Load Densities in Ion Exchange Chromatography Using an Asymmetric Activity Coefficient. *Biotechnol. J.* **2017**, *12*, 1600336. [CrossRef]
47. Joshi, M.; Seidel-Morgenstern, A.; Kremling, A. Exploiting the Bootstrap Method for Quantifying Parameter Confidence Intervals in Dynamical Systems. *Metab. Eng.* **2006**, *8*, 447–455. [CrossRef] [PubMed]
48. Kalyanaraman, J.; Kawajiri, Y.; Realff, M.J. Bayesian Design of Experiments for Adsorption Isotherm Modeling. *Comput. Chem. Eng.* **2020**, *135*, 106774. [CrossRef]
49. Ker, A.P.; Tolhurst, T.N.; Liu, Y. Bayesian Estimation of Possibly Similar Yield Densities: Implications for Rating Crop Insurance Contracts. *Am. J. Agric. Econ.* **2016**, *98*, 360–382. [CrossRef]
50. Pagel, M.; Meade, A.; Barker, D. Bayesian Estimation of Ancestral Character States on Phylogenies. *Syst. Biol.* **2004**, *53*, 673–684. [CrossRef]
51. Conrad, P.R.; Davis, A.D.; Marzouk, Y.M.; Pillai, N.S.; Smith, A. Parallel Local Approximation MCMC for Expensive Models. *SIAM-ASA J. Uncertain. Quantif.* **2018**, *6*, 339–373. [CrossRef]
52. He, Q.; Zhao, L. Bayesian Inference Based Process Design and Uncertainty Analysis of Simulated Moving Bed Chromatographic Systems. *Sep. Purif. Technol.* **2020**, *246*, 116856. [CrossRef]
53. Kitagawa, G. Monte Carlo Filter and Smoother for Non-Gaussian Nonlinear State Space Models. *J. Comput. Graph. Stat.* **1996**, *5*, 1–25. [CrossRef]
54. Kalyanaraman, J.; Kawajiri, Y.; Lively, R.P.; Realff, M.J. Uncertainty Quantification via Bayesian Inference Using Sequential Monte Carlo Methods for CO_2 Adsorption Process. *AIChE J.* **2016**, *62*, 3352–3368. [CrossRef]
55. Yamamoto, Y.; Yajima, T.; Kawajiri, Y. Uncertainty Quantification for Chromatography Model Parameters by Bayesian Inference Using Sequential Monte Carlo Method. *Chem. Eng. Res. Des.* **2021**, *175*, 223–237. [CrossRef]
56. Grosfils, V.; Levrie, C.; Kinnaert, M.; Wouwer, A. Vande A Systematic Approach to SMB Processes Model Identification from Batch Experiments. *Chem. Eng. Sci.* **2007**, *62*, 3894–3908. [CrossRef]

57. Draper, N.R. *Applied Regression Analysis*; McGraw-Hill. Inc: New York, NY, USA, 1998; ISBN 0471170828.
58. Antos, D.; Seidel-Morgenstern, A. Application of Gradients in the Simulated Moving Bed Process. *Chem. Eng. Sci.* **2001**, *56*, 6667–6682. [CrossRef]
59. Hoff, P.D. *A First Course in Bayesian Statistical Methods*; Springer: New York, NY, USA, 2009; Volume 580, ISBN 0387922997.
60. Gao, M.; Zhang, H. Sequential Monte Carlo Methods for Parameter Estimation in Nonlinear State-Space Models. *Comput. Geosci.* **2012**, *44*, 70–77. [CrossRef]
61. Goodfellow, I. *Deep Learning*; The MIT Press: Cambridge, MA, USA, 2016; ISBN 0262035613.
62. Akaike, H. A New Look at the Statistical Model Identification. *IEEE Trans. Automat. Contr.* **1974**, *19*, 716–723. [CrossRef]
63. Schwarz, G. Estimating the Dimension of a Model. *Ann. Stat.* **1978**, *6*, 461–464. [CrossRef]
64. Schiesser, W.E. *The Numerical Method of Lines: Integration of Partial Differential Equations*; Elsevier: Amsterdam, The Netherlands, 2012; ISBN 0128015519.
65. Lam, S.K.; Pitrou, A.; Seibert, S. Numba: A LLVM-Based Python Jit Compiler. In Proceedings of the Second Workshop on the LLVM Compiler Infrastructure in HPC, Austin, TX, USA, 15 November 2015; pp. 1–6.

Disclaimer/Publisher's Note: The statements, opinions and data contained in all publications are solely those of the individual author(s) and contributor(s) and not of MDPI and/or the editor(s). MDPI and/or the editor(s) disclaim responsibility for any injury to people or property resulting from any ideas, methods, instructions or products referred to in the content.